Performance Analysis of Hybrid SCM/OSCDM System using the Khazani-Syed (KS) Code

R. K. Z. SAHBUDIN, M. K. ABDULLAH
Department of Computer and Communication System Engineering,
Faculty of Engineering, University Putra Malaysia
43400 Serdang, Selangor
MALAYSIA
ratna@eng.upm.edu.my http://www.eng.upm.edu.my

Abstract: - This paper proposes a hybrid subcarrier multiplexing/optical spectrum code division multiplexing (SCM/OSCDM) system for the purpose of combining the advantages of both techniques. Optical spectrum code division multiple access (OSCDMA) is one of the multiplexing techniques that is becoming popular because of the flexibility in the allocation of channels, ability to operate asynchronously, enhanced privacy and increased capacity in bursty nature networks. On the other hand, subcarrier multiplexing (SCM) technique is able to enhance the channel data rate of OSCDMA systems. The system utilizes a new unified code construction named KS (Khazani-Syed) code based on the Double Weight (DW) and Modified Double Weight (MDW) codes. This paper also presents a new detection technique called Spectral Direct Decoding (SDD) detection technique for the OSCDM. SDD is effective in rejecting the unwanted signals that interfere with the wanted signals. This results in reduced receiver complexity and improved the performance of the hybrid system significantly.

Key-Words: - Hybrid SCM/OSCDM, Khazani-Syed (KS) code, multiple access interference, phase-induced intensity noise

1 Introduction

The SCM technology is simple and also cost effective. It provides a way to take advantage of the multi-gigahertz bandwidth of the fiber optics using well established microwave techniques for which components are matured and commercially available [1]. Furthermore it is less expensive than the corresponding wavelength division multiplexing (WDM) technology [2].

Optical CDMA (OCDMA) systems have received more attention because CDMA allows many users share the same transmission medium asynchronously and simultaneously with a high level of transmission security [3]. However, multiple access interference (MAI) is the main reason for performance degradation in OCDMA especially when large number of users is involved.

In this paper, the performance of the hybrid SCM/OSCDM system is investigated and presented. The system utilizes KS (Khazani-Syed) code which is a unified code construction based on DW and MDW codes [4]. This hybrid system is proposed for the purpose of combining the advantages of both techniques. It is proposed as a means of increasing the maximum permissible number of simultaneous active users by increasing the SCM and/or the OSCDMA codeword. Thus the resulting hybrid system is robust against interference, possesses high transmission security and increases the channel capacity in the existing optical fibers. In addition, a new detection technique named spectral direct decoding (SDD) is proposed for the hybrid system of SCM/OSCDM. It is a simple and an easy to build OSCDMA decoder, giving results better than the AND subtraction [5, 6] detection techniques. This new technique has reduced the receiver complexity and at the same time improved the system performance.

2 Hybrid SCM/OSCDM System

Fig. 1 shows the block diagram of the hybrid SCM/OSCDM system. At the transmitter, data with independent unipolar digital signal is mixed by a different microwave carrier. The subcarriers are combined and optically modulated onto the code sequence using an optical external modulator (OEM). Then m modulated code sequences are combined together and transmitted through the optical fiber. At the receiver, an optical splitter is

used to separate the different modulated code sequences. The received signal can be decoded by using a matched code sequence and the unmatched components will be filtered out. Then, the decoded signal is detected by the photodetector. A splitter and an electrical bandpass filter (BPF) are used to split the subcarrier multiplexed signals and to reject the unwanted signals, respectively. In order to recover the original transmitted data, the incoming signal is electrically mixed with a local microwave frequency f_i and filtered using low-pass filter (LPF).

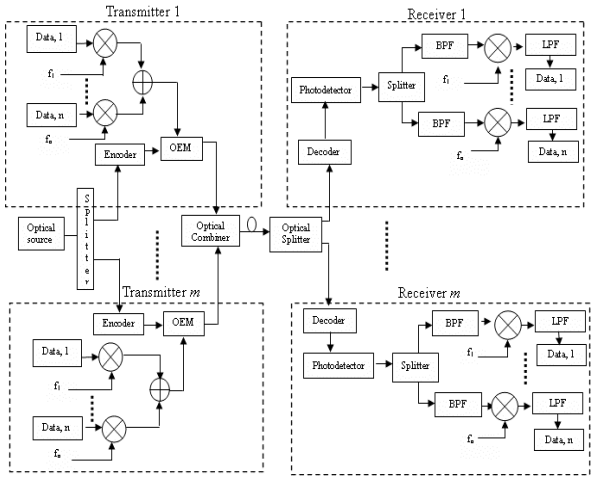

Fig. 1 Block Diagram of SCM/OSCDM System with Direct Decoding Technique

In this hybrid system, each user is assigned a particular code sequence c_i, and subcarrier frequency f_i, where the pair of (c_i, f_i) is unique with respect to every other user. Only the intended receiver is able to correctly demodulate the detected signal, made possible by the decoding scheme. Every receiver is matched to a pair of (c_i, f_i). Each receiver must tune to the correct frequency and code sequence to receive the desired data. Other signals are rejected.

2.1 AND Subtraction Detection Technique

The implementation of a hybrid SCM/OSCDM system using AND subtraction detection technique is shown in Fig. 2. Optical bandpass filters are used as the encoders and decoders for all detection techniques that will be discussed in this paper. For example, let us consider the KS code sequences as shown in Table 1.

Table 1. KS code with weight, W=2

	CODE SEQUENCE			
	λ_1	λ_2	λ_3	λ_4
X	1	1	0	0
Y	0	1	1	0

Note that λ_i where i is 1, 2, ...N, represents the spectral position of the chips in the KS code sequence.

The optical pulses are encoded according to the KS code sequence and then the code is optically modulated with the SCM signal. For example, the KS code sequences shown in Fig. 2 are denoted as X= (1100) and Y= (0110). The outputs of the two OEMs are combined and transmitted through an optical fiber.

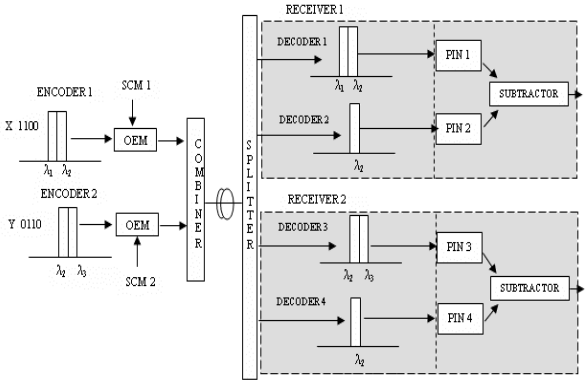

Fig. 2 Hybrid SCM/OSCDM System using AND Subtraction Technique

The outputs from the filters are detected by the two photodetectors (PIN) connected to a subtractor. In order to decode two code sequences of KS code and detect the signal, this technique requires four filters and four photodetectors. Two filters with bandwidth twice the chip width for λ_1 and λ_2, and λ_2 and λ_3, and two filters at the position of the overlapping spectra occurring in the code sequences, that is λ_2.

2.2 Spectral Direct Decoding (SDD) Detection Technique

The hybrid SCM/OSCDM system using SDD detection technique is illustrated in Fig. 3. This technique is simple and different as compared to the AND subtraction detection technique. For two KS code sequences as shown in Fig. 3, it requires only two filters for the decoders, which are used to filter the non-overlapping chips, λ_1 and λ_3 because the overlapping chips of the two code sequences may cause interference at the receiver [7]. The number of photodetectors is reduced to two. It does not require any subtractor at the receiver.

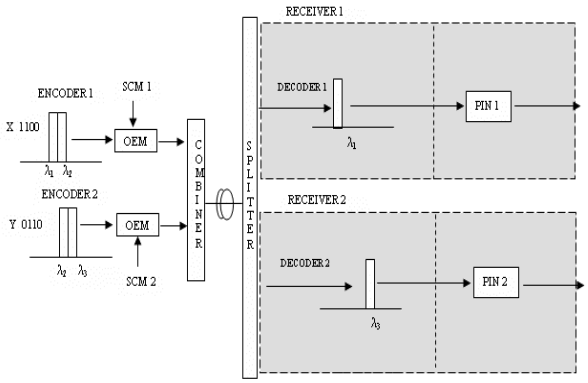

Fig. 3 Hybrid SCM/OSCDM System using SDD Detection Technique

3 Analysis of Hybrid SCM/OSCDM System

In the analysis of the proposed hybrid system, incoherent intensity noise, shot noise, thermal noise and inter-modulation distortion of subcarrier channels in both photodetectors are being considered. PIN photodetectors are used and the dark current is assumed negligible. The spacing of optical carriers is assumed to be sufficiently wide so that the effect of crosstalk from adjacent optical channels is negligible [8]. The subcarrier channels are equally spaced. In the analysis, the following assumptions are made [9, 10]:

i. The light source spectra is ideally unpolarized and its spectrum is flat over the bandwidth [ν_o-$\Delta\nu/2$, ν_o+$\Delta\nu/2$], where ν_o is the optical center frequency and $\Delta\nu$ is the optical source bandwidth in Hertz.
ii. Each power spectral component has identical spectral width.
iii. Each user has equal power at the receiver.
iv. Each bit stream from each user is synchronized.

The above assumptions are important so that the system performance can be easily analyzed using Gaussian approximation. Gaussian approximation is used for the calculation of bit error rate (BER) because it models quite accurately the noises and disturbances that always present in communication systems [11, 12]. Many researchers have used similar assumptions in their analysis [9, 13]. The noise variance of the photocurrent due to the detection can be denoted as:

$$\left\langle i^2 \right\rangle = \left\langle \mathrm{I}_{\mathrm{shot}}^2 \right\rangle + \left\langle \mathrm{I}_{\mathrm{PIIN}}^2 \right\rangle + \left\langle \mathrm{I}_{\mathrm{thermal}}^2 \right\rangle + \left\langle \mathrm{I}_{\mathrm{IMD}}^2 \right\rangle \qquad (1)$$

where $\mathrm{I}_{\mathrm{shot}}$ denotes the shot noise, $\mathrm{I}_{\mathrm{PIIN}}$ is the phase-induced intensity noise (PIIN), $\mathrm{I}_{\mathrm{thermal}}$ is the thermal noise and $\mathrm{I}_{\mathrm{IMD}}$ is the inter-modulation distortion noise of subcarrier channels.

3.1 Hybrid System Based AND Subtraction Technique

When incoherent light fields are mixed and incident upon a photodetector, the phase noise of the fields causes an intensity noise term in the photodetector output.

The source coherence time τ_c is expressed as [10, 12]:

$$\tau_c = \frac{\int_0^\infty G^2(v)\,dv}{\left[\int_0^\infty G(v)\,dv\right]^2} \qquad (2)$$

where $G(v)$ is the power spectral density (PSD) of the thermal source.

If $\mathrm{C}_k(i)$ denotes the ith element of the kth KS code sequence, the code properties for AND subtraction technique can be written as:

$$\sum_{i=1}^{N} \mathrm{C}_k(i)\mathrm{C}_l(i) = \begin{cases} \mathrm{W}, \text{ For } k = l \\ 1, \quad \text{For } k \neq l \\ 0, \quad \text{For } k \neq l \end{cases} \begin{matrix} \text{in the same sector} \\ \\ \text{not in the same sector} \end{matrix} \qquad (3)$$

and

$$\sum_{i=1}^{N} \mathrm{C}_k(i)\left(\mathrm{C}_l(i) \bullet \mathrm{C}_k(i)\right) = \begin{cases} 1, \text{For} \quad k = l \\ 1, \text{For} \quad k \neq l \\ 0, \text{For} \quad k \neq l \end{cases} \begin{matrix} \text{in the same sector} \\ \\ \text{not in the same sector} \end{matrix} \qquad (4)$$

The condition of k and l in the same sector meaning that both code sequences are in **C(1), C(2)** or **C(M)** as shown in Fig. 4. And for the condition of k and l not in the same sector meaning that one of the code sequence might be in **C(1)** and the other code sequence is in **C(2)** or **C(M).**

$$\mathbf{C(m)} = \begin{bmatrix} \mathbf{C(1)} & 0 & 0 & 0 \\ 0 & \mathbf{C(2)} & 0 & 0 \\ 0 & 0 & \ddots & 0 \\ 0 & 0 & 0 & \mathbf{C(M)} \end{bmatrix}$$

Fig. 4 Mapping Technique of the KS Code

The matrix size of each 0 and **C(m),** 1< m ≤ M is the same as **C(1)** matrix size. For a fixed value of weight, when the number of mapping is increased, the code size is extended by (m x K_B) and the basic code is extended diagonally as shown in Fig. 4. K_B is the basic code's row size which is also known as the basic number of codes, given by:

$$K_B = \frac{\mathrm{W}}{2} + 1 \qquad (5)$$

The AND operation of [$\mathrm{C}_l(i)$•$\mathrm{C}_k(i)$] is valid for $k \neq l$ only. However the cross correlation of

$C_k(i)[C_l(i)\bullet C_k(i)]$ is valid for $k = l$ and $k \neq l$. From Equation (3), the cross correlation of $C_k(i)C_l(i)$ is W when $k = l$. The MAI can be eliminated as the cross correlation $\sum_{i=1}^{N} C_k(i)\left(C_l(i)\bullet C_k(i)\right)$ can be subtracted from $C_k(i)C_l(i)$ when $k \neq l$. The subtraction can be derived as:

$$\sum_{i=1}^{N} C_k(i)C_l(i) - \sum_{i=1}^{N} C_k(i)\left(C_l(i)\bullet C_k(i)\right) = \begin{cases} W-1, & k=l \\ 0, & k\neq l \end{cases} \quad (6)$$

Hence, the weight is zero when $k \neq l$, meaning MAI can be fully removed by using AND subtraction detection technique.

The PSD of the received optical signals can be written as [14]:

$$r(v)=\frac{P_{sr}}{\Delta v}\sum_{k=1}^{N_w} d_k \sum_{i=1}^{N} c_k(i)\,\mathrm{rect}(i) \quad (7)$$

where P_{sr} is the effective power of a broad-band source at the receiver, N_w is the number KS optical code sequences, each carrying their corresponding subcarrier. N is the KS code length. $d_k(t)$ represents the modulated data of nth subcarrier channel on the kth optical code expressed as

$$d_k(t) = \sum_{n=1}^{N_c} u_{n,k}(t)m_{n,k}\cos(\omega_n t) \quad (8)$$

$u_{n,k}(t)$ is the normalized digital signal at the nth subcarrier channel of the kth code, where 0 and 1 are represented as digital signal "0" and "1", respectively. ω_n is the angular subcarrier frequency, $m_{n,k}$ is the modulation index of the nth subcarrier of the kth code and N_c is the number of subcarrier channels on each code. Assuming an identical modulation index for all subcarrier channels, it is necessary that $0 < m_{n,k} \leq \frac{1}{N_c}$ [15].

The rect (i) function in Equation (7) is given by:

$$\mathrm{rect}(i) = u\left[\nu-\nu_o-\frac{\Delta\nu}{2N}(-N+2i-2)\right]-u\left[\nu-\nu_o-\frac{\Delta\nu}{2N}(-N+2i)\right]$$
$$= u\left[\frac{\Delta\nu}{N}\right] \quad (9)$$

where $u(v)$ is the unit step function expressed as:

$$u(v) = \begin{cases} 1, & v \geq 0 \\ 0, & v < 0 \end{cases} \quad (10)$$

The total power incident at the input of PIN 1 and PIN 2 of Fig. 2 is given by:

$$\int_0^\infty G_1(\nu)d\nu = \int_0^\infty \left[\frac{P_{sr}}{\Delta\nu}\sum_{k=1}^{N_w} d_k(t)\sum_{i=1}^{N} C_k(i)C_l(i)\left\{u\left[\frac{\Delta\nu}{N}\right]\right\}\right]d\nu$$

$$\int_0^\infty G_1(\nu)d\nu = \frac{P_{sr}}{\Delta\nu}\frac{\Delta\nu}{N}\sum_{k=1}^{N_w} d_k(t)\sum_{i=1}^{N} C_k(i)C_l(i)$$

$$\int_0^\infty G_1(\nu)d\nu = \frac{P_{sr}W}{N}d_l + \frac{P_{sr}}{N}\sum_{k=1,k\neq l}^{N_w} d_k \quad (11)$$

and

$$\int_0^\infty G_2(\nu)d\nu = \int_0^\infty \left[\frac{P_{sr}}{\Delta\nu}\sum_{k=1}^{N_w} d_k(t)\sum_{i=1}^{N} C_k(i)\left(C_l(i)\bullet C_k(i)\right)\left\{u\left[\frac{\Delta\nu}{N}\right]\right\}\right]d\nu$$

$$\int_0^\infty G_2(\nu)d\nu = \frac{P_{sr}}{\Delta\nu}\frac{\Delta\nu}{N}\sum_{k=1}^{N_w} d_k(t)\sum_{i=1}^{N} C_k(i)\left(C_l(i)\bullet C_k(i)\right)$$

$$\int_0^\infty G_2(\nu)d\nu = \frac{P_{sr}}{N}d_l + \frac{P_{sr}}{N}\sum_{k=1,k\neq l}^{N_w} d_k \quad (12)$$

Consequently, the signal from the desired user is given by the difference of the photodiode current ***I***, expressed as:

$$\boldsymbol{I} = \boldsymbol{I_1} - \boldsymbol{I_2} \quad (13)$$

where

$\boldsymbol{I_1}$, $\boldsymbol{I_2}$ = current at PIN1 and PIN2, respectively.

$$\boldsymbol{I} = \Re\int_0^\infty G_1(\nu)\,d\nu - \Re\int_0^\infty G_2(\nu)\,d\nu$$
$$= \Re\left[\int_0^\infty G_1(\nu)d\nu - \int_0^\infty G_2(\nu)d\nu\right]$$
$$= \frac{\Re P_{sr}(W-1)}{N}\sum_{n=1}^{N_c} u_{n,k}(t)m_{n,k}\cos(\omega_n t) \quad (14)$$

where $\Re$ is the responsivity of the photodetectors given by :

$$\Re = \frac{\eta e}{h\nu_c} \quad (15)$$

Here, η is the quantum efficiency, e is the electron's charge, h is the Plank's constant, and ν_c is the central frequency of the original broadband optical pulse.

The useful photocurrent signal for the kth channel can be found as:

$$\boldsymbol{I} = \frac{\Re P_{sr}(W-1)}{N}\sum_{n=1}^{N_c} u_{n,k}(t)m_{n,k}\cos(\omega_n t) \quad (16)$$

At the RF demodulator, the signal coherently mixes with a local oscillator 2 $\cos(\omega_n t)$.

$$\boldsymbol{I} = \frac{\Re P_{sr}(W-1)}{N}\sum_{n=1}^{N_c} u_{n,k}(t)m_{n,k}\cos(\omega_n t)\left[2\cos(\omega_n t)\right]$$
$$= \frac{\Re P_{sr}(W-1)}{N}\sum_{n=1}^{N_c} u_{n,k}(t)m_{n,k}\left[2\cos^2(\omega_n t)\right] \quad (17)$$

Using the trigonometric identities, $\boldsymbol{I}$ becomes

$$\boldsymbol{I} = \frac{\Re P_{sr}(W-1)}{N}\sum_{n=1}^{N_c} u_{n,k}(t)m_{n,k}\left[1+\cos(2\omega_n t)\right] \quad (18)$$

The frequency-doubled component is filtered out using LPF and therefore the output of the demodulator is

$$\boldsymbol{I} = \frac{\Re P_{sr}(W-1)}{N}m_{n,k}u_{n,k}(t) \quad (19)$$

The noise power of shot noise can be written as:

$$\left\langle \mathrm{I}_{\mathrm{shot}}^2 \right\rangle = 2e\mathrm{B}(\boldsymbol{I_1} + \boldsymbol{I_2})$$

$$= 2e\,\mathrm{B}\,\Re\left[\int_0^\infty G_1(v)dv + \int_0^\infty G_2(v)dv\right]$$

$$= 2e\mathrm{B}\Re\left[\frac{\Delta v}{N}\right]\cdot\left[\frac{\mathrm{P_{sr}W}}{\Delta v}+\frac{\mathrm{P_{sr}}}{\Delta v}\sum_{k=1}^{N_w}\sum_{k\neq l}\mathrm{d}_k+\frac{\mathrm{P_{sr}}}{\Delta v}+\frac{\mathrm{P_{sr}}}{\Delta v}\sum_{k=1}^{N_w}\sum_{k\neq l}\mathrm{d}_k\right]$$

$$= 2e\mathrm{B}\Re\left[\frac{\Delta v}{N}\right]\cdot\left[\frac{\mathrm{P_{sr}}}{\Delta v}\right]\left[\mathrm{W}+\sum_{k=1}^{N_w}\sum_{k\neq l}\mathrm{d}_k+1+\sum_{k=1}^{N_w}\sum_{k\neq l}\mathrm{d}_k\right]$$

$$= 2e\mathrm{B}\Re\cdot\left[\frac{\mathrm{P_{sr}}}{N}\left(\mathrm{W}+1+\left(K_B-1\right)+\left(K_B-1\right)\right)\right] \quad (20)$$

Hence, Equation (20) is the shot noise for the hybrid system using AND subtraction detection technique. It can be simplified by substituting Equation (5) in Equation (20). The simplified equation is given as:

$$\left\langle \mathrm{I}_{\mathrm{shot}}^2 \right\rangle = 2e\mathrm{B}\Re\cdot\left[\frac{\mathrm{P_{sr}}}{N}\left(2\mathrm{W}+1\right)\right] \quad (21)$$

By using the methodology similar to that in [13] and approximating the summation $\sum_{k=1}^{N_w}\mathrm{C}_k(i)\cong\frac{N_w\mathrm{W}}{N}$ and the noise power of PIIN can be written as:

$$\left\langle I_{\mathrm{PIIN}}^2 \right\rangle = \mathrm{B}\,\boldsymbol{I_1^2}\,\tau_{c1} + \mathrm{B}\,\boldsymbol{I_2^2}\,\tau_{c2}$$

$$= \mathrm{B}\,\Re^2\left[\int_0^\infty G_1^2(v)dv + \int_0^\infty G_2^2(v)dv\right]$$

$$= \mathrm{B}\Re^2\frac{\mathrm{P_{sr}^2}}{N\Delta\mathrm{v}}\sum_{i=1}^{N}\left\{\mathrm{C}_l(i)\cdot\left[\sum_{k=1}^{N_w}\mathrm{d}_k\mathrm{C}_k(i)\right]\cdot\left[\sum_{m=1}^{N_w}\mathrm{d}_m\mathrm{C}_m(i)\right]\right\}$$

$$+\mathrm{B}\Re^2\frac{\mathrm{P_{sr}^2}}{N\Delta\mathrm{v}}\sum_{i=1}^{N}\left\{\left(\mathrm{C}_l(i)\bullet\mathrm{C}_k(i)\right)\left[\sum_{k=1}^{N_w}\mathrm{d}_k\mathrm{C}_k(i)\right]\cdot\left[\sum_{m=1}^{N_w}\mathrm{d}_m\mathrm{C}_m(i)\right]\right\}$$

$$\cong\frac{\mathrm{B}\Re^2\mathrm{P_{sr}^2}}{N\Delta\mathrm{v}}\sum_{i=1}^{N}\left\{\mathrm{C}_l(i)\frac{N_w\mathrm{W}}{N}\cdot\left[\sum_{k=1}^{N_w}\mathrm{C}_k(i)\right]\right\}$$

$$+\frac{\mathrm{B}\Re^2\mathrm{P_{sr}^2}}{N\Delta\mathrm{v}}\sum_{i=1}^{N}\left\{\left(\mathrm{C}_l(i)\bullet\mathrm{C}_k(i)\right)\frac{N_w\mathrm{W}}{N}\cdot\left[\sum_{k=1}^{N_w}\mathrm{C}_k(i)\right]\right\}$$

$$\cong\frac{\mathrm{B}\Re^2\mathrm{P_{sr}^2}}{N\Delta\mathrm{v}}\frac{N_w\mathrm{W}}{N}\sum_{k=1}^{N_w}\left[\sum_{i=1}^{N}\mathrm{C}_k(i)\mathrm{C}_l(i)\right]$$

$$+\frac{\mathrm{B}\Re^2\mathrm{P_{sr}^2}}{N\Delta\mathrm{v}}\frac{N_w\mathrm{W}}{N}\sum_{k=1}^{N_w}\left[\sum_{i=1}^{N}\mathrm{C}_k(i)\left(\mathrm{C}_l(i)\bullet\mathrm{C}_k(i)\right)\right]$$

$$=\mathrm{B}\Re^2\left[\frac{\mathrm{P_{sr}^2}}{N\Delta\mathrm{v}}\right]\left[\frac{N_w\mathrm{W}}{N}\right]\left[\mathrm{W}+\left(K_B-1\right)+1+\left(K_B-1\right)\right]$$

$$=\mathrm{B}\,\Re^2\left[\frac{\mathrm{P_{sr}^2}\,N_w\,\mathrm{W}}{N^2\Delta v}\right]\left[\,\mathrm{W}+1+\left(2K_B-2\right)\,\right] \quad (22)$$

Substitute Equation (5) in Equation (22), therefore the PIIN noise can be written as:

$$=\mathrm{B}\,\Re^2\left[\frac{\mathrm{P_{sr}^2}\,N_w\,\mathrm{W}}{N^2\Delta v}\right]\left(2\mathrm{W}+1\right) \quad (23)$$

The thermal noise is given as [16]:

$$\left\langle I_{thermal}^2 \right\rangle = \frac{4\mathrm{K}_b\mathrm{T}_n\mathrm{B}}{\mathrm{R}_L} \quad (24)$$

The inter-modulation distortion noise is given as [17, 18]:

$$\left\langle I_{\mathrm{IMD}}^2 \right\rangle = \mathrm{P_{sr}}^2\Re^2\,m_{n,k}^6\left[\frac{D_{111}}{32}+\frac{D_{21}}{128}\right] \quad (25)$$

where D_{111} is the three-tone third order inter-modulation at $\mathrm{f_i} + \mathrm{f_k} - \mathrm{f_l}$, D_{21} is the two-tone third order inter-modulation at $2\mathrm{f_i} - \mathrm{f_k}$.

The SNR of the hybrid system can be written as:

$$\mathrm{SNR} = \frac{(I_1-I_2)^2}{\left\langle I^2\right\rangle} \quad (26)$$

Noting that the probability of sending bit '1' at any time for each user is a $\frac{1}{2}$ [13],

$$\mathrm{SNR} = \frac{\Re^2\mathrm{P_{sr}}^2\,(\mathrm{W}-1)^2\,m_{n,k}^2}{N^2}$$

$$\frac{e\mathrm{B}\Re\mathrm{P_{sr}}}{N}\left[2\mathrm{W}+1\right]+\frac{\mathrm{B}\Re^2\mathrm{P_{sr}}^2N_w\,\mathrm{W}}{2N^2\Delta v}\left[2\mathrm{W}+1\right]+\frac{4\mathrm{K}_b\mathrm{T}_n\mathrm{B}}{\mathrm{R}_L}+\mathrm{P_{sr}^2}\Re^2m_{n,k}^6\left[\frac{D_{111}}{32}+\frac{D_{21}}{128}\right] \quad (27)$$

3.2 Hybrid System Based SDD Technique

The setup of the hybrid system using SDD technique is depicted in Fig. 3. This technique is simple and the number of filters at the decoders is reduced. The code properties for the KS code using this technique is also different compared with the system using the subtraction detection techniques.

If $\mathrm{C}_k(i)$ denotes the *i*th element of the *k*th KS code sequence, the code properties for SDD detection technique can be written as:

$$\sum_{i=1}^{N}\mathrm{C}_k(i)\mathrm{C}_l(i) = \begin{cases}\dfrac{\mathrm{W}}{2}, & For \quad k=l\\ 0, & For \quad k\neq l\end{cases} \quad (28)$$

The condition of *k* and *l* is as mentioned earlier.

In this technique the PSD at the input of PIN 1 as in Fig. 3 of the *l*th receiver during one data bit period can be written as $G_{dd}(v)$. Using the same mathematical operation as in the previous section, $G_{dd}(v)$ can be written as:

$$G_{dd}(v)dv = \frac{\mathrm{P_{sr}}}{\Delta v}\sum_{k=1}^{N_w}\mathrm{d}_k(t)\sum_{i=1}^{N}\mathrm{C}_k(i)\mathrm{C}_l(i)\left\{\mathrm{u}\left[\frac{\Delta v}{N}\right]\right\} \quad (29)$$

The total power incident at the input of photodetector is given as:

$$\int_0^{\infty} G_{dd}(v)dv = \int_0^{\infty} \frac{P_{sr}}{\Delta v} \sum_{k=1}^{N_w} d_k(t) \sum_{i=1}^{N} C_k(i) C_l(i) \left\{ u\left[\frac{\Delta v}{N} \right] \right\} dv$$

$$\int_0^{\infty} G_{dd}(v)dv = \frac{P_{sr}}{\Delta v} \frac{\Delta v}{N} \sum_{k=1}^{N_w} d_k(t) \sum_{i=1}^{N} C_k(i) C_l(i)$$

$$\int_0^{\infty} G_{dd}(v)dv = \frac{P_{sr} W}{2N} d_l \quad (30)$$

The signal from the desired user is given by the photodiode current $\boldsymbol{I}$, which can be written as:

$$\boldsymbol{I} = \boldsymbol{I_{dd}} = \Re \int_0^{\infty} G_{dd}(v)\, dv \quad (31)$$

Substitute Equation (30) in Equation (31),

$$\boldsymbol{I} = \Re \left[\frac{P_{sr}}{N} \right] \cdot \left[\frac{W}{2} d_l \right] \quad (32)$$

In SDD detection technique, only the non-overlapping chips are filtered. This is because the overlapping chip of the two code sequences may cause interference at the receiver [7, 19]. Therefore the desired signal for this technique is:

$$\boldsymbol{I} = \Re \left[\frac{P_{sr}}{N} \right] \cdot \left[\frac{W}{2} d_l \right]$$

$$= \frac{\Re P_{sr} W}{N2} \sum_{n=1}^{N_c} u_{n,k}(t) m_{n,k} \cos(\omega_n t) \quad (33)$$

The useful photocurrent signal for the kth channel can be found as:

$$\boldsymbol{I} = \frac{\Re P_{sr} W}{N2} \sum_{n=1}^{N_c} u_{n,k}(t) m_{n,k} \cos(\omega_n t) \quad (34)$$

At the RF demodulator, the signal coherently mixes with a local oscillator and is filtered by the LPF. Thus the output of the demodulator is

$$\boldsymbol{I} = \frac{\Re P_{sr} W}{N2} m_{n,k} u_{n,k}(t) \quad (35)$$

Since only the non-overlapping chip is filtered for SDD technique, PIIN noise is not considered. PIIN noise occurs only when more than one optical signal is incident on the photodetector surface [20, 21]. The total noise here is considered to be only the sum of shot noise, thermal noise and inter-modulation distortion noise, which is expressed as:

$$\langle I^2 \rangle = 2eB(I_{dd}) + \frac{4K_b T_n B}{R_L} + P_{sr}^2 \Re^2 m_{n,k}^6 \left[\frac{D_{111}}{32} + \frac{D_{21}}{128} \right] \quad (36)$$

Substituting I_{dd} in Equation (36) gives,

$$\langle I^2 \rangle = 2eB\Re \left[\int_0^{\infty} G_{dd}(v)dv \right] + \frac{4K_b T_n B}{R_L} + P_{sr}^2 \Re^2 m_{n,k}^6 \left[\frac{D_{111}}{32} + \frac{D_{21}}{128} \right] \quad (37)$$

Note that the probability of sending bit '1' at any time for each user is ½, thus Equation (37) becomes

$$\langle I^2 \rangle = eB\Re \cdot \left[\frac{P_{sr}}{N} \left(\frac{W}{2} \right) \right] + \frac{4K_b T_n B}{R_L} + P_{sr}^2 \Re^2 m_{n,k}^6 \left[\frac{D_{111}}{32} + \frac{D_{21}}{128} \right] \quad (38)$$

The SNR of the hybrid system using the SDD detection technique can be determined using the same mathematical operations as in previous section without the PIIN, where it can be expressed as:

$$\text{SNR} = \frac{(I_{dd})^2}{\langle I^2 \rangle} \quad (39)$$

SNR=

$$\frac{\frac{\Re^2 P_{sr}^2 \left(\frac{W}{2} \right)^2 m_{n,k}^2}{N^2}}{\frac{eB\Re P_{sr}}{N} \left[\frac{W}{2} \right] + \frac{4K_b T_n B}{R_L} + P_{sr}^2 \Re^2 m_{n,k}^6 \left[\frac{D_{111}}{32} + \frac{D_{21}}{128} \right]} \quad (40)$$

Hence, MAI and PIIN are eliminated due to the fact that only optical signals without interference are incident on the photodetector's surface.

4 Results

To ensure a fair comparison of the performances of the hybrid systems, this study uses the same parameters as those adopted in [22-24]. The typical parameters used in the analysis are listed in Table 2. The performances of the system are characterized by referring to BER and the effects of number of users.

Table 2. Typical parameters used in the analysis

Symbol	Parameter	Value
η	Photodetector Quantum efficiency	0.6
Δv	Line-width Broadband Source	3.75 THz
λ_o	Operating Wavelength	1550 nm
B	Electrical Bandwidth	311 MHz
R_b	Data Bit Rate	622 Mbps
T_n	Receiver Noise Temperature	300 K
R_L	Receiver Load Resistor	1030 Ω
e	Electron Charge	1.6×10^{-19} C
h	Planck's Constant	6.66×10^{-34} Js
K_b	Bolzmann's Constant	1.38×10^{-23} J/K

Fig. 5 shows the performance comparison between the hybrid system using SDD and AND subtraction detection techniques for various number of subcarriers when P_{sr} = -10 dBm. The number of KS codes is purposely set at 2 in order to observe the

effect of the number of subcarriers on the hybrid system performance.

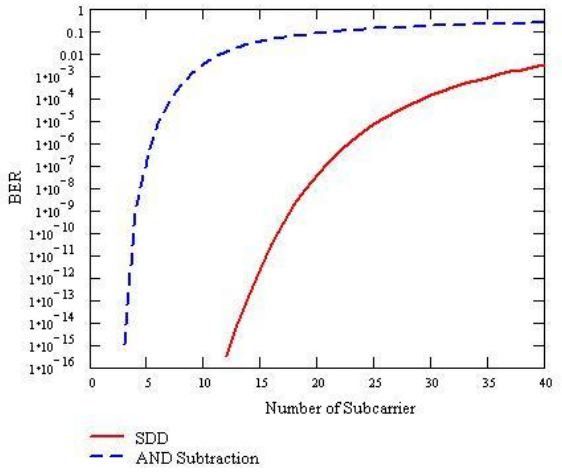

Fig. 5 BER versus Number of Subcarriers for the Hybrid System at P_{sr} = -10 dBm

Observation on Fig. 5 reveals that with the weight of 4 for KS code, there is a limitation on the number of subcarriers from the BER (maximum 10^{-9}) point of view. The number of subcarriers with an acceptable BER for the system using SDD and AND subtraction techniques are less than 17 and 4, respectively. The BER for the system using SDD technique is better compared to that using the AND subtraction technique. The BER degrades as the number of subcarriers increases. This is because the optical modulation index per subcarrier decreases linearly with the number of channels. Thus increases the BER of the system.

The performance of the hybrid system using SDD technique with different weights is depicted in Fig. 6 when P_{sr} = -10 dBm. When P_{sr} = -10 dBm or greater, the inter-modulation distortion noise is the main noise. By looking at Equation (40), the effect when P_{sr} increases is not as great as when a bigger code weight is used. With a bigger code weight, not only the total number of users is significantly increased, but also a better performance of the hybrid system results. Fig. 6 shows that the total number of users to maintain an acceptable BER for the system with W = 4 and W = 6 are less than 52 and 78, respectively. Note that this condition is achieved when other parameters are not changed.

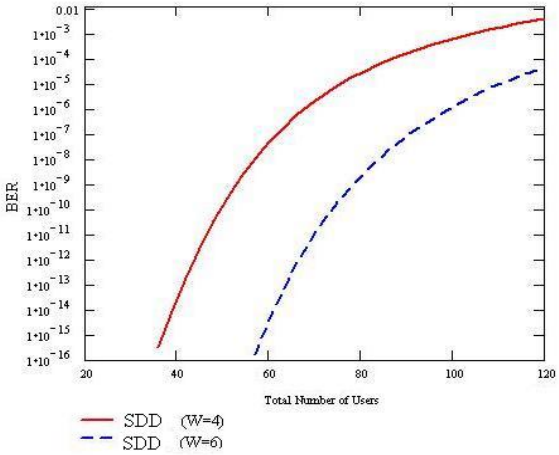

Fig. 6 BER versus Total Number of Users for the Hybrid System at P_{sr} = -10 dBm

The system capacity versus total number of simultaneous users is depicted in Fig. 7. The network capacity is determined by the possible number of simultaneous users multiplied by the bit rate per user [10, 25, 26]. In this figure the system performance requirement is BER = 10^{-9}. It is clear that as the number of simultaneous users increases, the hybrid system using the SDD technique is more bandwidth efficient than that using the AND subtraction technique.

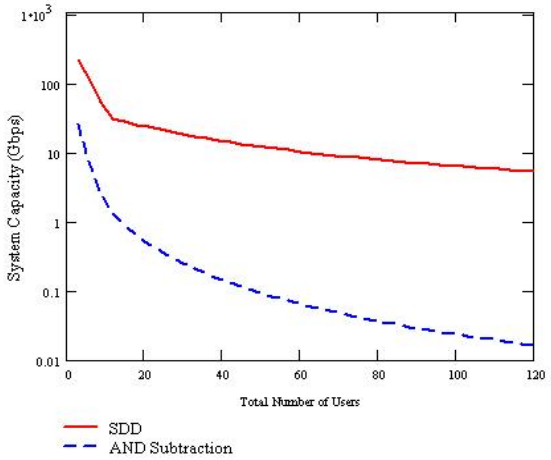

Fig. 7 System Capacity versus Total Number of Simultaneous Users When the Required BER is 10^{-9}

5 Conclusion

In this paper, a new detection technique for the OSCDM of the hybrid system and the detailed system performance analysis has been presented. It has been proven that the performance of hybrid

system using the new detection technique is improved significantly as the PIIN and MAI are totally eliminated. Hence, it can accommodate more users to access the network simultaneously. The complexity of the overall system is also reduced with the reduced number of filters and photodetectors required for the SDD detection technique.

References:

[1] P. Laurencio, S. O. Simoes and M. C. R. Medeiros, Impact of the Combined Effect of RIN and Intermodulation Distortion on OSSB/SCM Systems, *Journal of Lightwave Technology*, Vol. 24, No. 11, 2006, pp. 4250-4262.

[2] T. E. Thomas, and K. Bala, *Multiwavelength Optical Networks: A Layered Approach*, Addison Wesley Longman, 1999.

[3] J. C. Palais, Fiber *Optic Communications*, Fifth Edition, Pearson Prentice Hall, 2005.

[4] M. K. Abdullah, S. A. Aljunid, S. B. A. Anas, R. K. Z. Sahbudin, M. Mokhtar, A New Optical Spectral Amplitude Coding Sequence: Khazani-Syed (KS) Code, *Proceeding of International Conference on Information and Communication Technology (ICICT '07),* 2007, pp. 266-278.

[5] S. A. Aljunid, S. Zarihan, M. S. Anuar, M. N. Junita, A. Norsuhaida, M. D. A. Samad, and M. K. Abdullah, Improving Bit Error Rate OCDMA Systems using AND Subtraction Technique, *Proceeding of International RF and Microwave Conference*, 2006, pp. 334-337.

[6] S. A. Aljunid, F. N. Hasson, M. D. A. Samad, M. K. Abdullah, M. Othman, and S. Shaari, Performance of OCDMA Systems using AND Subtraction Technique, *Proceeding of IEEE International Conference on Semiconductor Electronics*, 2006, pp. 464-467.

[7] P. Kamath, J.D. Touch, and J.A. Bannister, Algorithms for Interference Sensing in Optical CDMA Networks, *IEEE International Conference on Communications,* Vol.3, 2004, pp.1720– 1724.

[8] L. Chao, Effect of Laser Diode Characteristics on the Performance of an SCM-OFDM Direct Detection System, *IEE Proceedings J. Optoelectronics,* Vol. 140, Issue 6, 1993, pp. 392 – 396.

[9] J. H. Wen, J. S. Jhou and C. P. Li, Optical Spectral Amplitude Coding CDMA Systems using Perfect Difference Codes and Interference Estimation", *IEE Proceeding of Optoelectronics,* Vol. 153, No. 4, 2006, pp. 152-160.

[10] E. D. J. Smith, R. J. Blaikie and D. P. Taylor, Performance Enhancement of Spectral-Amplitude-Coding Optical CDMA using Pulse-Position Modulation", *IEEE Transactions on Communications,* Vol. 46, No. 9, 1998, pp. 1176-1184.

[11] L. Kazovsky, S. Benedetto, and A. Willner, *Optical Fiber Communication Systems,* Artech House, Inc., 1996.

[12] C.-H. Lin, J. Wu, H.-W. Tsao, C.-L. Yang, Spectral Amplitude-Coding Optical CDMA System using Mach-Zehnder Interferometers, *IEEE Journal of Lightwave Technology,* Vol. 23, No. 4, 2005, pp. 1543-1553.

[13] C.-M. Tsai, Optical Wavelength/Spatial Coding System Based on Quadratic Congruence Code Matrices, *IEEE Photonics Technology Letters*, Vol. 18, No. 17, 2006, pp. 1843-1845.

[14] C.-C. Yang, J.-F. Huang and S.-P. Tseng, Optical CDMA Network Codecs Structured with M-Sequence Codes over Waveguide-Grating Routers, *IEEE Photonics Technology Letters*, Vol. 16, No. 2, 2004, pp. 641-643.

[15] R. Hui, B. Zhu, R. Huang, C. T. Allen, K. R. Demarest, and D. Richards, Subcarrier Multiplexing for High Speed Optical Transmission, *Journal of Lightwave Technology*, Vol. 20, No. 3, 2002, pp. 417-427.

[16] R. Papannareddy, *Introduction to Lightwave Communication Systems*, Artech House, Inc, 1997.

[17] B. J. Koshy, P. M. Shankar, Efficient Modeling and Evaluation of Fiber-fed Microcellular Networks in a Land Mobile Channel using a GMSK Modem Scheme, *IEEE Journal on Selected Areas in Communications*, Vol. 15, No. 4, 1997, pp. 694-705.

[18] B. J. Koshy and P. M. Shankar, Spread Spectrum Techniques for Fiber-fed Microcellular Networks, *IEEE Transactions on Vehicular Technology,* Vol. 48, No. 3, 1999, pp. 847- 857.

[19] P. Kamath, J. D. Touch, J. A. Bannister, Algorithms for Transmission Scheduling in Optical CDMA Networks, *ISI-TR-2006-617*, 2006, pp. 1-14.

[20] M. M. Rad and J. A. Salehi, Phase-induced Intensity Noise in Digital Incoherent All-Optical Tapped-delay Line Systems, *Journal of Lightwave Technology*, Vol. 24, No. 8, 2006, pp. 3059-3072.

[21] J. Capmany, B. Ortega, and D. Pastor, A Tutorial on Microwave Photonic Filters,

Journal of Lightwave Technology, Vol. 24, No. 1, 2006, pp. 201-229.

[22] Z. Wei, H. G. Shiraz, Codes for Spectral-amplitude-coding Optical CDMA Systems, *IEEE Journal of Lightwave Technology*, Vol. 20, No. 8, 2002, pp. 1284-1291.

[23] Z. Wei, H. Ghafauri-Shiraz, Unipolar Codes with Ideal In-phase Cross-correlation for Spectral-amplitude-coding Optical CDMA Systems, *IEEE Transactions on Communications*, Vol. 50, No. 8, 2002, pp. 1209-1212.

[24] Z. Wei, H. Ghafauri-Shiraz and H. M. H. Shalaby, Performance Analysis of Optical Spectral-amplitude-coding CDMA Systems using a Super-fluorescent Fiber Source, *IEEE Photonics Technology Letters*, Vol. 13, No. 8, 2001, pp. 887-889.

[25] Z. Wei, H. Ghafauri-Shiraz, Unipolar Codes with Ideal In-phase Cross-correlation for Spectral-amplitude-coding Optical CDMA Systems, *IEEE Transactions on Communications*, Vol. 50, No. 8, 2002, pp. 1209-1212.

[26] T. Demeechai, On Noise-limited Performance of Noncomplementary Spectral-amplitude coding Optical CDMA Systems, *IEEE Transactions on Communications,* Vol. 54, Issue 1, 2006, pp. 29- 31.